American Mineralogist, Volume 94, pages 622–625, 2009

LETTER

Determination of the crystal structure of sanderite, $MgSO_4 \cdot 2H_2O$, by X-ray powder diffraction and the charge flipping method

HONGWEI MA,[1,*] DAVID L. BISH,[1] HSIU-WEN WANG,[1] AND STEVE J. CHIPERA[2]

[1]Department of Geological Sciences, Indiana University, 1001 East 10th Street, Bloomington, Indiana 47405, U.S.A.
[2]Chesapeake Energy Corporation, 6100 N. Western Avenue, Oklahoma City, Oklahoma 73118, U.S.A.

ABSTRACT

The crystal structure of sanderite, $MgSO_4 \cdot 2H_2O$, was determined from laboratory X-ray powder diffraction data measured from 2–140 °2θ using Cu*K*α radiation. Sanderite is orthorhombic, space group $P2_12_12_1$, with unit-cell parameters a = 8.8932(1) Å, b = 8.4881(1) Å, c = 12.4401(2) Å, V = 939.16(3) Å^3, Z = 8. The crystal structure model was determined using the charge flipping method and was refined using fundamental parameters Rietveld refinement method to R_{wp} = 6.52%, R_{exp} = 1.89%, and χ^2 = 3.43. Bond-valence calculations for the refined model show that the structure is chemically reasonable. In the refined structure, Mg^{2+} cations are coordinated by four O atoms from $[SO_4]^{2-}$ groups and by two H_2O molecules, forming distorted octahedra. By sharing vertex O atoms, $[SO_4]$ tetrahedra and $[MgO_4(H_2O)_2]$ octahedra build up a 3-D framework.

Keywords: Sanderite, $MgSO_4 \cdot 2H_2O$, crystal structure, charge flipping, structure determination, powder diffraction

INTRODUCTION

Magnesium sulfate hydrates have many hydration states and are stable over a variety of conditions on the Earth's surface. Mg-sulfates have been also suggested as important martian surface phases since the time of the Viking landers, and recent chemical and spectroscopic data provide further support for the occurrence of a variety of hydrated Mg-sulfate minerals on the surface of Mars (Vaniman et al. 2004; Bibring et al. 2005; Gendrin et al. 2005; Chipera and Vaniman 2007; Mangold et al. 2008). In addition, recent orbital measurements have shown a heterogeneous distribution of H over the Martian surface, with up to ~10% H_2O-equivalent H, some or all of which may occur in the form of hydrated minerals (Feldman et al. 2003; Bish et al. 2003; Feldman et al. 2004). Crystal structures and stability relations for the $MgSO_4 \cdot nH_2O$ series are necessary to infer, which species can exist on the martian surface and how much water they may contain if present (Bish et al. 2003; Chipera and Vaniman 2007). The crystal structures of the $MgSO_4 \cdot nH_2O$ series for n = 1 (kieserite, Aleksovska et al. 1998), 4 (starkeyite, Baur 1964), 5 (pentahydrite, Baur and Rolin 1972), 6 (hexahydrite, Zalkin et al. 1964), 7 (epsomite, Calleri et al. 1984), and 11 (meridianiite, Peterson et al. 2007) have been determined. Sanderite (n = 2) was discovered over 50 years ago and is a well-defined synthetic phase. It occurs with hexahydrite, pentahydrite, and starkyite in marine salt deposits (Berdesinki 1952) and as an efflorescence on Neogene rocks in Greece (Schnitzer 1977). The IMA currently lists sanderite with questionable status as a mineral. Lallemant and Watelle-Marion (1967a, 1967b) synthesized the two-hydrate $MgSO_4$ and provided X-ray powder diffraction data. However, its crystal structure has not been determined (Jambor et al. 2000). In this communication, we describe the solution of the sanderite crystal structure from X-ray powder diffraction data measured on a synthetic sample.

EXPERIMENTAL METHODS

Sanderite was prepared by maintaining ultrapure reagent-grade hexahydrite in temperature-relative humidity (RH) field for sanderite, bypassing the formation of other intermediate hydrates. As sanderite *T*-RH conditions are significantly outside the stability field for hexahydrite, the solid first transformed into an amorphous phase from which sanderite subsequently crystallized. To prepare the sample used for structure determination, hexahydrite was placed onto a heating stage in a controlled-environment cell on the powder X-ray diffractometer and heated to 75 °C in a 50% RH nitrogen atmosphere (RH determined at 23 °C, Chipera et al. 1997). The effective % RH at 75 °C is ~5% RH. As shown by a sequence of X-ray diffraction (XRD) measurements over 240 h, hexahydrite rapidly reacted to an amorphous phase from which sanderite slowly crystallized. After the final measurement of this sequence, XRD data were measured on a cavity-mounted specimen from 2–140 °2θ (0.02° steps, 20 s/step count time) using a Siemens D500 with Cu*K*α radiation, incident- and diffracted-beam Soller slits, and a Kevex PSi solid-state detector. The final sanderite diffraction pattern included a trace of the 2.4 hydrate that initially formed when hexahydrite transformed to the amorphous phase. We also measured the XRD pattern of the 2.4 hydrate, and this pattern was used to correct for the small amount of the 2.4 hydrate evident in the sanderite pattern, through manual subtraction using a modified version of the FullPat software (Chipera and Bish 2002).

Thermogravimetric analysis (TGA) was conducted using ~15 mg of sanderite prepared by placing hexahydrite in a 75 °C oven for 10 days at ambient room RH (18–28% RH), equivalent to ~2.5% RH at 75 °C. This sample contained a trace (1–3%) of the 2.4 hydrate. The TGA data showed a weight loss of ~37%, corresponding to ~2.2 H_2O molecules/unit cell. The reason for the discrepancy between this amount and the theoretical value may be due to admixture with the small amount of the 2.4 H_2O phase.

* E-mail: hongma@indiana.edu

RESULTS AND DISCUSSION

Unit cell, space group, and unit-cell contents

Thirty diffraction peaks below 45 °2θ were selected and indexed using the single-value-decomposition method (Coelho 2003) implemented in TOPAS Academic 4.1 (Coelho 2007). The result was confirmed by indexing the pattern with TREOR (Werner and Eriksson et al. 1985) and ITO (Visser 1969). Refined unit-cell parameters from TREOR are a = 8.8943(9) Å, b = 8.4880(9) Å, c = 12.4404(14) Å, α = 90°, β = 90°, γ = 90°, with M(30) = 20, F(30) = 38 where M(30) and F(30) are the de Wolf figures of merit and the F index, respectively. This unit cell accounted for all 30 peaks. Diffraction intensities for each reflection were obtained using Le Bail profile fitting (Le Bail et al. 1988) in the program TOPAS, and the final R_{wp} for the Le Bail fit was 5.6%. Observed extinction conditions were *hkl*: no limits; *h*00: h = 2n; 0*k*0: k = 2n; 00*l*: l = 2n. The space group was thus definitely determined to be $P2_12_12_1$ (no. 19), also in agreement with the possible space group(s) suggested by the indexing programs. Based on thermal analyses and literature data (Berdesinki 1952; Lallemant and Watelle-Marion 1967a, 1967b), the probable formula for sanderite is $MgSO_4{\cdot}2H_2O$. Based on eight sanderite "molecules" in the unit cell, the calculated density is 2.21 g/cm^3, consistent with measured and calculated densities in the $MgSO_4{\cdot}nH_2O$ series. Appendix 1[1] contains bond lengths, angles, and CIF information for the refined sanderite structure.

Structure determination by the charge flipping method

Structure determination from powder diffraction data (SDPD) (David et al. 2006) has developed over the last 30 years from an art to an almost-routine technique and a powerful alternative when samples are available only as crystalline powders. Charge flipping (Oszlanyi and Suto 2004, 2005) is one of the latest tools whereby the phase problem is solved by an iterative procedure involving both real and reciprocal space perturbations instead of statistical phase relations. It is a dual-space method that switches back and forth between real and reciprocal space. The first application of charge flipping to the solution of crystal structures from powder diffraction data were presented by Wu et al. (2006).

Both real space and reciprocal space perturbation were applied to determine the structure of sanderite. Perturbations in reciprocal space included setting the data resolution to 1.0 Å. Observed reflections above the threshold were deleted and 30 missing reflections below 1.0 Å were generated and treated as weak reflections. There are 603 unique reflections over the angular range of measurement, including the 30 missing reflections. Of these 603 reflections, 329 were set to be weak. During each iteration, amplitudes of the weak reflections were maintained while a π/2 phase shift was randomly added to 1/3 of the weak reflections. In real space, electron densities were modified in the following way. First,

$$\rho = \begin{cases} -\rho & \text{if } \rho \in \text{the lowest 75\%} \\ \min(\rho, 0.5{*}\rho_{max}) & \text{if } \rho \in \text{the highest 25\%} \end{cases}$$

Second, the origin of the unit cell was located in each iteration and electron densities were shifted to a position that best matched the symmetry. In addition, an inexact but sufficiently strong symmetry restraint was applied to the flipped electron density pixels so that they followed the space group symmetry. Third, the charge flipping loop was interrupted if the R factor did not decrease for 100 consecutive iterations, and then random phases in the range of (–π, π) were given to the structure factor amplitudes to begin a new cycle. Fourth, the 559 E values (normalized structure factors) were used for the tangent formula and 50 triplets were set up for each reflection. The solution was found with R = 0.397 after 690 iterations within 7 s. The R factor contrast is ~0.10, a value sufficient for determining the structure solution. All independent non-hydrogen atoms and their equivalents were located, but no effort was made to determine the location of hydrogen atoms.

Rietveld refinement and structure validation

The structure model from charge flipping was refined using the fundamental parameters Rietveld approach implemented in TOPAS-Academic (Coelho 2007). Fundamental parameters for this refinement were determined from the instrumental parameters and by measuring reference materials and refining associated parameters, which were then fixed during the Rietveld refinement for sanderite. Two peaks in the region of 98.4~99.2 and 115.8~116.8 °2θ known to be from the sample holder were excluded. The background was modeled by a six-order Chebyshev polynomial. Scale factor, unit-cell parameters, and atomic coordinates were refined and occupancy factors were fixed. Representative atomic displacement factors were fixed for groups of similar atoms. Soft constraints were applied to the $[SO_4]$ tetrahedra and Mg-O distances, and these constraints were used throughout refinement. Other refined parameters include specimen displacement, crystallite size and strain, and preferred orientation. The final Rietveld refinement converged to R_{wp} = 6.52% with χ^2 = 3.44, and the results are shown in Table 1. Bond valence summations (Brown 1992) were calculated to evaluate the refined model, although contributions from H atoms could not be included. The calculated bond valence sums for unique atoms (except H_2O) in the unit cell are: Mg1 2.15, Mg2 2.16, S1 5.74, S2 5.95, O1 1.88, O2 1.78, O3 1.78, O4 1.76, O5 1.73, O6 1.91, O7 1.96, and O8 1.89, in agreement with the expected oxidation states of these elements in the structure.

Structure description

Crystallographically independent atoms in the sanderite unit cell include two Mg^{2+} cations, two $[SO_4]^{2-}$ groups, and two H_2O molecules. Each Mg^{2+} is coordinated by two H_2O molecules and four O atoms from four $[SO_4]^{2-}$ groups, and each $[SO_4]^{2-}$ group shares its four O atoms with four Mg cations. Thus, the structure of sanderite consists of a three-dimensional (3-D) framework

[1] Deposit item AM-09-020, Appendix 1 and CIF. Deposit items are available two ways: For a paper copy contact the Business Office of the Mineralogical Society of America (see inside front cover of recent issue) for price information. For an electronic copy visit the MSA web site at http://www.minsocam.org, go to the American Mineralogist Contents, find the table of contents for the specific volume/issue wanted, and then click on the deposit link there.

made of corner-sharing $[MgO_4(H_2O)_2]$ octahedra and $[SO_4]$ tetrahedra (Fig. 1). As shown in Table 1, the average Mg-O distance is 2.06 Å, the average Mg-H_2O length is slightly longer, with an average value of 2.11 Å, and the average S-O distance in the $[SO_4]^{2-}$ group is 1.48 Å. These values are in agreement with values reported for the structures of other members of the $MgSO_4{\cdot}nH_2O$ series and those in other sulfate minerals in general (Hawthorne et al. 2000). Bond angles (see supporting materials) indicate that $[MgO_4(H_2O)_2]$ octahedra are distorted, whereas the $[SO_4]$ tetrahedra deviate only slightly from ideal geometry.

The structures of all members of the $MgSO_4{\cdot}nH_2O$ series consist of $[SO_4]$ tetrahedra and $[Mg(O,H_2O)_6]$ octahedra, but each member has a unique structure due to variations in the topological arrangements of these polyhedra. The number of H_2O molecules changes the coordination environments of Mg^{2+} cations and the linkages of polyhedra, giving rise to different crystal structures for all of the different hydrated Mg-sulfates. Transitions between all of the different hydrated states of Mg-sulfate are reconstructive, with the exception of the reversible transition from epsomite to hexahydrite (and back), which involves the loss (gain) of an H_2O molecule. This structural complexity thus complicated the determination of the structure of sanderite. In the $MgSO_4{\cdot}nH_2O$ series, Mg^{2+} can coordinate with two (n = 1, 2), four (n = 4, 5), or six (n = 6, 7, 11) water molecules. Other corners of the Mg-octahedra are occupied by O atoms of the sulfate groups. The $[SO_4]$ groups can share four (n = 1,2), two (n = 4,5), or zero (n = 6,7,11) apices with Mg-octahedra. With an increase in the number of H_2O molecules, Mg^{2+} cations are coordinated by fewer O atoms of the sulfate groups and more H_2O molecules that typically do not bridge polyhedra. As a result, the structural topology of the $MgSO_4{\cdot}nH_2O$ series decreases from a three-dimensionally infinite framework (n = 1,2), through finite clusters (n = 4) and infinite chains (n = 5), to isolated sulfate tetrahedra and Mg-octahedra (n = 6,7,11). Water molecules either coordinate to a Mg^{2+} cation or simply function as interstitial molecules (n = 5,7,11). Only in kieserite do the H_2O molecules bridge two Mg-octahedra (n = 1). On the other hand, H-bonds play increasingly important roles in building the structures as more H_2O molecules occupy the structure. The finite clusters (n = 4), infinite chains (n = 5), and isolated polyhedra (n = 6,7,11) in the structure of the $MgSO_4{\cdot}nH_2O$ series are linked by H-bonds, involving H-bonds between Mg-octahedra and S-tetrahedra, together with weak H-bonds between adjacent like polyhedra and those within the clusters. However, the 3-D framework structures of kieserite and sanderite (n = 1,2) are formed by corner-sharing $[Mg(O,H_2O)_6]$ octahedra and $[SO_4]$ tetrahedra. There are possible H_2O-H_2O H-bonds and interactions between the H_2O molecules and other O atoms. It is likely that these H-bonds stabilize the crystal structure, but the importance of H-bonds in sanderite is not as obvious as in the structures of other members of this series.

TABLE 1. Atomic coordinates, equivalent isotropic displacement parameters (Å²) and selected bond lengths (Å) for sanderite

Atom	*x*	*y*	*z*	B_{eq}
Mg1	0.7870(2)	0.4648(2)	0.2552(1)	0.8
Mg2	0.2976(2)	0.5404(2)	0.4961(2)	0.8
S1	0.1435(2)	0.5737(2)	0.2508(1)	0.4
S2	0.6641(2)	0.5816(2)	0.4898(1)	0.4
O1	0.1492(8)	0.7382(3)	0.2126(3)	1.2
O2	0.2656(4)	0.5499(7)	0.3322(2)	1.2
O3	0.1676(7)	0.4614(5)	0.1597(2)	1.2
O4	0.0012(3)	0.5415(7)	0.3076(4)	1.2
O5	0.7345(5)	0.4598(5)	0.4171(2)	1.2
O6	0.7578(5)	0.7231(3)	0.4804(4)	1.2
O7	0.6596(6)	0.5135(5)	0.5978(2)	1.2
O8	0.5089(3)	0.6171(6)	0.4561(4)	1.2
O1w	0.5628(3)	0.4006(8)	0.2188(5)	1.2
O2w	0.7150(7)	0.6989(4)	0.2377(4)	1.2
O3w	0.3569(8)	0.3027(4)	0.4753(4)	1.2
O4w	0.0691(3)	0.4779(7)	0.5115(5)	1.2

Mg1-O1[a]	2.044(4)	Mg2-O2	2.060(4)	S1-O1	1.475(3)	S2-O5 1.509(4)
Mg1-O4[b]	2.096(4)	Mg2-O3[d]	2.058(3)	S1-O2	1.498(4)	S2-O6 1.466(4)
Mg1-O5	2.067(4)	Mg2-O6[e]	2.058(3)	S1-O3	1.496(4)	S2-O7 1.463(3)
Mg1-O7[c]	2.023(3)	Mg2-O8	2.049(4)	S1-O4	1.493(4)	S2-O8 1.473(4)
Mg1-O1w	2.116(4)	Mg2-O3w	2.101(4)			
Mg1-O2w	2.099(4)	Mg2-O4w	2.109(4)			

Notes: Symmetry transformations used to generate equivalent atoms: (a) $-x+1, y-1/2, -z+½$, (b) $x+1, y, z$, (c) $-x+3/2, -y+1, z-½$, (d) $-x+1/2, -y+1, z+½$, (e) $x-1/2, -y+3/2, -z+1$.

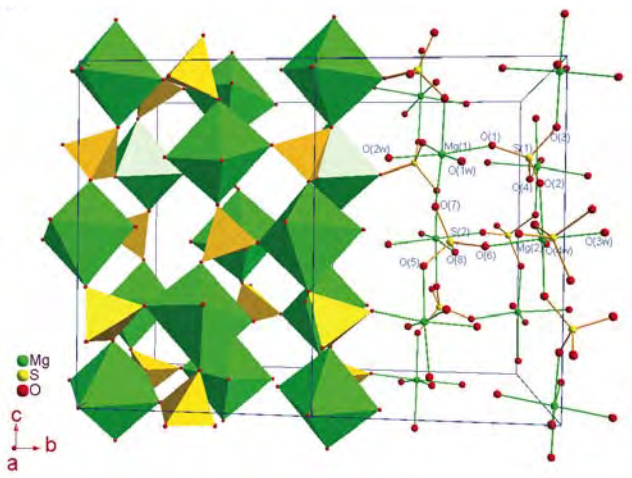

FIGURE 1. Crystal structure of sanderite. (Color online)

ACKNOWLEDGMENTS

This research was funded in part by a NASA Mars Fundamental Research grant, no. NNG06GH40G, to D.L.B.

REFERENCES CITED

Aleksovska, S., Petrusevski, V.M., and Soptrajanov, B. (1998) Calculation of structural parameters in isostructural series: the kieserite group. Acta Crystallographica, B54, 564–567.

Baur, W.H. (1964) On the crystal chemistry of salt hydrates. II. A neutron diffraction study of $MgSO_4(H_2O)_4$. Acta Crystallographica, 17, 863–869.

Baur, W.H. and Rolin, J.L. (1972) Salt hydrates. IX. The comparison of the crystal structure of magnesium sulfate pentahydrate with copper sulfate pentahydrate and magnesium chromate pentahydrate. Acta Crystallographica, 28, 1448–1455.

Berdesinki, W. (1952) Sanderite, leonhardtite, allenite and hexahydrite, new minerals of marine salts deposits. Neues Jahrbuch für Mineralogie-Monatshefte, 28–29.

Bibring, J.-P., Langevin, Y., Gendrin, A., Gondet, B., Poulet, F., Berthe, M., Soufflot, A., Arvidson, R., Mangold, N., Mustard, J., Drossart, P., and the OMEGA Team (2005) Mars surface diversity as revealed by the OMEGA/Mars Express observations. Science, 307, 1576–1581.

Bish, D.L., Carey, J.W., Vaniman, D.T., and Chipera, S.J. (2003) Stability of hydrous minerals on the Martian surface. Icarus, 164, 96–103.

Brown, I.D. (1992) Chemical and steric constraints in inorganic solids. Acta Crystallographica, B48, 553–572.

Calleri, M., Gavetti, A., Ivaldi, G., and Rubbo, M. (1984) Synthetic epsomite, $MgSO_4(H_2O)_7$: Absolute configuration and surface features of the complementary (111) forms. Acta Crystallographica, B40, 218–222.

Chipera, S.J. and Bish, D.L. (2002) FULLPAT: a full-pattern quantitative analysis program for X-ray powder diffraction using measured and calculated patterns. Journal of Applied Crystallography, 35, 744–749.

Chipera, S.J. and Vaniman, D.T. (2007) Experimental stability of magnesium sulfate hydrates that may be present on Mars. Geochimica et Cosmochimica Acta, 71, 241–250.

Chipera, S.J., Carey, J.W., and Bish, D.L. (1997) Controlled-humidity XRD analyses: application to the study of smectite expansion/contraction. In J.V. Gilfrich, I.C. Noyan, R. Jenkins, T.C. Huang, R.L. Snyder, D.K. Smith, M.A. Zaitz, and P.K. Predecki, Eds., Advances in X-Ray Analysis, 39, p. 713–722. Plenum Press, New York.

Coelho, A.A. (2003) Indexing of powder diffraction patterns by iterative use of singular value decomposition. Journal of Applied Crystallography, 36, 86–95.

——— (2007) TOPAS-Academic V4.1 Technical reference. http://members.optusnet.com.au/alancoelho.

David, W.I.F., Shankland, K., McCusker, L.B., and Baerlocher, C. (2006) Structure Determination from Powder Diffraction Data, p. 252–285. Oxford University Press, U.K.

Feldman, W.C., Prettyman, T.H., Maurice, S., Plaut, J.J., Bish, D.L., Vaniman, D.T., Mellon, M.T., Metzger, A.E., Squyres, S.W., Karunatillake, S., Boynton, W.V., Elphic, R.C., Funsten, H.O., Lawrence, D.J., and Tokar, R.L. (2003) Global distribution of near-surface hydrogen on Mars. Journal of Geophysical Research, 109, E09006.

Feldman, W.C., Mellon, M.T., Maurice, S., Prettyman, T.H., Carey, J.W., Vaniman, D.T., Bish, D.L., Fialips, C.I., Chipera, S.J., Kargel, J.S., Elphic, R.C., Funsten, H.O., Lawrence, D.J., and Tokar, R.L. (2004) Hydrated states of $MgSO_4$ at equatorial latitudes on Mars. Geophysical Research Letters, 31, L16702.

Gendrin, A., Mangold, N., Bibring, J.-P., Langevin, Y., Gondet, B., Poulet, F., Bonello, G., Quantin, C., Mustard, J., Arvidson, R., and LeMouelic, S. (2005) Sulfates in Martian layered terrains: the OMEGA/Mars Express view. Science, 307, 1587–1591.

Hawthorne, F.C., Krivovichev, S.V., and Burns, P.C. (2000) The crystal chemistry of sulfate minerals. In C.N. Alpers, J.L. Jambor, and D.K. Nordstrom, Eds., Sulfate Minerals: Crystallography, Geochemistry and Environmental Significance, 40, p. 1–101. Reviews in Mineralogy and Geochemistry, Mineralogical Society of America, Chantilly, Virginia.

Jambor, J.L., Nordstrom, D.K., and Alpers, C.N. (2000) Metal-sulfate salts from sulfide mineral oxidation. In C.N. Alpers, J.L. Jambor, and D.K. Nordstrom, Eds., Sulfate Minerals: Crystallography, Geochemistry and Environmental Significance, 40, p. 303–350. Reviews in Mineralogy and Geochemistry, Mineralogical Society of America, Chantilly, Virginia.

Lallemant, M. and Watelle-Marion, G. (1967a) Dégradation thermique du sulfate de magnésium heptahydraté sous pression de vapeur d'eau contrôlée. Mécanisme observé de 10^{-3} à 40 torr. Comptes rendus des séances de l'Académie des sciences, Paris, Série C, 264, 2030–2033.

——— (1967b) Dégradation thermique du sulfate de magnésium heptahydraté sous pression de vapeur d'eau contrôlée. Mécanisme observé au-dessus de 50 torr. Comptes rendus des séances de l'Académie des sciences, Paris, Série C, 265, 627–630.

Le Bail, A., Duroy, H., and Fourquet, J.L. (1988) Ab initio structure determination of $LiSbWO_6$ by X-ray powder diffraction. Materials Research Bulletin, 23, 447–452.

Mangold, N., Gendrin, A., Gondet, B., LeMouelic, S., Quantin, C., Ansan, V., Bibring, J.-P., Langevin, Y., Masson, P., and Neukum, G. (2008) Spectral and geological study of the sulfate-rich region of West Candor Chasma, Mars. Icarus, 194, 519–543.

Oszlanyi, G. and Suto, A. (2004) Ab initio structure solution by charge flipping. Acta Crystallographica, A60, 134–141.

——— (2005) Ab initio structure solution by charge flipping. II. Use of weak reflections. Acta Crystallographica, A61, 147–152.

Peterson, R.C., Nelson, W., Madu, B., and Shurvell, H.F. (2007) Meridianiite: A new mineral species observed on Earth and predicted to exist on Mars. American Mineralogist, 92, 1756–1759.

Schnitzer, W.A. (1977) An unusual efflorescence (apowite) on Neogene rocks from the Ismuth of Corinth. Annales Geologiques des Pays Helleniques, 28, 349–351 (not seen, referenced in Jambor et al. 2000).

Vaniman, D.T., Bish, D.L., Chipera, S.J., Fialips, C.I., Carey, J.W., and Feldman, W.C. (2004) Magnesium sulfate salts and the history of water on Mars. Nature, 431, 663–665.

Visser, J.W. (1969) A fully automatic program for finding the unit cell from powder data. Journal of Applied Crystallography, 2, 89–95.

Werner, P.E., Eriksson, L., and Westdahl, M. (1985) TREOR, a semi-exhaustive trial-and-error powder indexing program. Journal of Applied Crystallography, 18, 367–370.

Wu, J.S., Leinenweber, K., Spence, J.C.H., and O'Keefe, M. (2006) Ab initio phasing of X-ray powder diffraction patterns by charge flipping. Nature Materials, 5, 647–652.

Zalkin, A., Ruben, H., and Templeton, D.H. (1964) The crystal structure and hydrogen bonding of magnesium sulfate hexahydrate. Acta Crystallographica, 17, 235–240.

MANUSCRIPT RECEIVED OCTOBER 8, 2008
MANUSCRIPT ACCEPTED DECEMBER 15, 2008
MANUSCRIPT HANDLED BY BRYAN CHAKOUMAKOS